

# Anisotropy of Magnetic Susceptibility (AMS) Characteristics of Tide-Influenced Sediments in the Late Pleistocene-Holocene Changjiang Incised-Valley Fill, China

Baozhu Liu<sup>†‡</sup>, Yoshiki Saito<sup>†</sup>, Toshitsugu Yamazaki<sup>†</sup>, Abdelaziz Abdeldayem<sup>†,††</sup>, Hirokuni Oda<sup>†</sup>, Kazuaki Hori<sup>‡‡</sup>, and Quanhong Zhao<sup>§</sup>

<sup>†</sup>IGG, Geological Survey of Japan  
AIST, Higashi 1-1-1, Tsukuba  
Ibaraki 305-8567, Japan  
bliuz@lsu.edu

<sup>‡</sup>Coastal Studies Institute  
Louisiana State University  
Baton Rouge, LA 70803, U.S.A.

<sup>††</sup>Geology Department  
Faculty of Science  
Tanta University  
Tanta 31527, Egypt

<sup>‡‡</sup>Department of Geography  
Graduate School of Science  
University of Tokyo  
Hongo 7-3-1, Bunkyo-ku  
Tokyo 113-0033, Japan

<sup>§</sup>Marine Geology Laboratory  
Tongji University  
1239 Siping Road  
Shanghai 200092, P.R. China

## ABSTRACT



LIU, B.; SAITO, Y.; YAMAZAKI, T.; ABDELDAYEM, A.; ODA, H.; HORI, K., and ZHAO, Q., 2005. Anisotropy of Magnetic Susceptibility (AMS) Characteristics of Tide-Influenced Sediments in the Late Pleistocene-Holocene Changjiang Incised-Valley Fill, China. *Journal of Coastal Research*, 21(5), 1031–1041. West Palm Beach (Florida). ISSN 0749-0208.12

In order to probe anisotropy of magnetic susceptibility (AMS) characteristics of tide-influenced sediments, AMS analyses and primary sedimentary structure observation and description were conducted on the borehole CM-97 samples from Changjiang delta, China. Primary sedimentary structure (cross-laminations) observation and description were based on a detailed examination of X-ray photographs of samples. Primary cross-laminations were found on 19 of 35 subcores, among which five subcores, A6, A7, B17, B30, and B38, have bidirectional cross-laminations. We found a total of 35 cross-laminations on the subcore sections of tide-influenced sediments, of which 14 were distributed on the five subcores with bidirectional cross-laminations. By their bidirectional dipping foreset laminae, the primary cross-laminations clearly showed bidirectional flow features of the environments in which these sediments formed. Comparing the paleocurrent directions shown by these cross-laminations with those indicated by the *in situ* AMS data, we found that more than 64% exhibited similar current directions, demonstrating that AMS can supply us with the true paleocurrent directions for such sediments. From the downhole paleocurrent changes inferred from the *in situ* AMS data, it was also clear that there were bidirectional flows during the deposition of these sediments and that sediments deposited in different environments had different change characteristics with respect to downhole paleocurrents. These differences among the muddy intertidal- to subtidal-flat sediments (unit 5), the Changjiang estuary central basin sediments (unit 6), and the delta front sediments (unit 8) may have resulted from the different hydrodynamic conditions of these sedimentary environments. Furthermore, stratigraphic unit 5 was subdivided into three parts based on downhole AMS characteristics, which may correlate with those subdivided according to downhole paleocurrent changes. Therefore, besides its long recognized role in paleocurrent determination, AMS can also be used to determine stratigraphic divisions and to reconstruct sedimentary paleoenvironments in detail.

**ADDITIONAL INDEX WORDS:** *Changjiang (Yangtze River) delta, anisotropy of magnetic susceptibility (AMS), tide-influenced, sedimentary structures, paleocurrent, cross-lamination.*

## INTRODUCTION

Any material acquires magnetization in a magnetic field and thus has magnetic susceptibility, which is not always isotropic but varies depending on the orientations of the rock (ISING, 1942). This spatial variation of the susceptibility is defined as the anisotropy of magnetic susceptibility (AMS), which reflects the preferred orientation of the magnetic minerals in rock or unconsolidated sediments, *i.e.*, its magnetic fabric (HROUDA, 1982; TARLING and HROUDA, 1993). AMS has long been demonstrated to be a useful tool in paleocurrent determination, in particular for deep-sea sediments such

as contourites (ABDELDAYEM *et al.*, 1999; ELLWOOD, 1980; ELLWOOD and LEDBETTER, 1977, 1979; ELLWOOD *et al.*, 1979; LEDBETTER and ELLWOOD, 1980; YOKOKAWA and FRANZ, 2002), turbidites (ELLWOOD and LEDBETTER, 1977; LEDBETTER and ELLWOOD, 1980), and submarine canyon and fan sediments (REES *et al.*, 1968). It has also been found useful in determining paleocurrents for mid-Proterozoic embayment shale (SCHIEBER and ELLWOOD, 1993), Palaeozoic flysch shale (PIPER *et al.*, 1996), modern beach sand sediments (REES, 1965; TAIRA and LIENERT, 1979), aeolian sediments (LAGROIX and BANERJEE, 2002), and laboratory-deposited sediments (REES, 1965; REES and WOODALL, 1975). AMS of experimental tidal flat sediments has also been reported elsewhere (ELLWOOD, 1984), and it has been demon-

strated that AMS is applicable for paleocurrent determination of sediments deposited in coastal estuary and delta environments (LIU *et al.*, 2001).

AMS can be illustrated by an ellipsoid with three axes, representing maximum ( $K_1$ ), intermediate ( $K_2$ ), and minimum susceptibility ( $K_3$ ) of the sample (TARLING and HROUDA, 1993). This ellipsoid resembles the shape of sediment grains. Generally, current direction is parallel to the direction (declination,  $D_1$ ) of maximum susceptibility (ABDELDAYEM *et al.*, 1999; REES, 1965; TARLING and HROUDA, 1993). Thus,  $D_1$  can be used to discuss current directions.

The Changjiang (Yangtze River) of China is the longest river in Asia, with a length of about 6,300 km, a total catchment area of about  $1.8 \times 10^6$  km<sup>2</sup>, mean annual runoff of  $893 \times 10^9$  m<sup>3</sup>, and mean annual sediment discharge of  $481 \times 10^6$  t (LI and WANG, 1998; MILLIMAN and MEADE, 1983). A huge incised valley formed during the Last Glacial Period and was filled up by river, estuary, and delta sediments during the postglacial sea-level rise (LI *et al.*, 2000). The present Changjiang delta, a typical example of tide-dominated delta, has been forming since the maximum Holocene transgression at about 7 kyr BP (LI and WANG, 1998; LI *et al.*, 2000; LIU *et al.*, 1992). At present, the Changjiang delta is in a meso- to macrotidal environment, with an average tidal range of 2.6 m and a maximum of about 5.0 m, flood-tidal currents directing to the northwest and ebb-tidal currents directing to the south-southeast (LI and WANG, 1998).

In this paper, we present further research results comparing sedimentary structures and AMS data, and we discuss downhole paleocurrent changes in borehole CM-97 as well as AMS characteristics of tide-influenced sediments of the Changjiang delta, China.

## MATERIALS AND METHODS

A 70-m-long borehole core, CM-97 (latitude 31°37'29"N, longitude 121°23'38"E; elevation 2.48 m; Figure 1), was drilled in 1997 on Chongming Island by rotary drilling using drilling mud. The borehole site was located in the incised valley that formed during the Last Glacial Period in the Changjiang estuary (Figure 1; LI *et al.*, 2000). Core recovery was about 90%. Borehole CM-97 consisted of 39 separate subcores, and all subcore samples were split lengthwise down the middle into two halves. A total of 2543 discrete samples were taken by continuously pressing standard 7-cm<sup>3</sup> plastic cubes into the face of the working half. A detailed core description and radiocarbon dates from the borehole are reported by HORI *et al.* (1999, 2001a, 2001b).

Borehole CM-97, covering the period between 11.5 and 1.5 kyr BP, has been divided into nine stratigraphic units (HORI *et al.*, 1999; Figure 2), of which units 2 to 9 were deposited in tide-influenced environments (HORI *et al.*, 2001a, 2001b). In terms of separate subcores, 35 out of 39 subcores consisted of tide-influenced estuarine or deltaic sediments. Samples for this study were from the tide-influenced subcores, especially subcores A7, B17, B30, and B38, which were deposited in tide-dominated environments (HORI *et al.*, 1999, 2001a, 2001b) and on which bidirectional primary sedimentary structures (cross-laminations) have been observed.

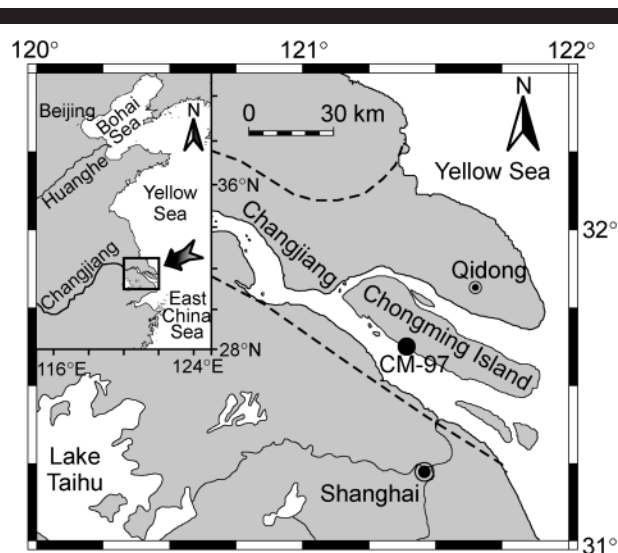


Figure 1. Location of borehole CM-97 and map of the Changjiang (Yangtze River) delta. The area between the two dashed lines shows the incised valley of the Changjiang, which formed during the Last Glacial Maximum (after LI *et al.*, 2000). The inset rectangle shows the location of the study area in China.

Initial low-field magnetic susceptibility ( $K$ ) and its anisotropy were first measured using a KappaBridge KLY-3S susceptibility meter. Following the recommendations of ELLWOOD *et al.* (1988), JELINEK (1981), and TARLING and HROUDA (1993), a set of AMS parameters that define mean magnetic susceptibility ( $K$ ), corrected anisotropy degree ( $P_j$ ), magnetic lineation ( $L$ ), magnetic foliation ( $F$ ), and the ellipsoid shape factor ( $q$ ) were calculated and used to evaluate the features of the magnetic fabric of the tide-influenced sediments as follows:

$$K = (K_1 + K_2 + K_3)/3$$

(Mean magnetic susceptibility, Nagata, 1961)

$$P_j = \exp \sqrt{2[(n_1 - n_m)^2 + (n_2 - n_m)^2 + (n_3 - n_m)^2]}$$

(Corrected anisotropy degree, Jelinek, 1981)

$$L = K_1/K_2$$

(Magnetic lineation,  
Balsley and Buddington, 1960)

$$F = K_2/K_3$$

(Magnetic foliation, Stacey *et al.*, 1960)

$$q = (K_1 - K_2)/[(K_1 + K_2)/2 - K_3]$$

(Shape factor, Granar, 1958)

Only the samples that satisfied primary magnetic fabric criteria (HAMILTON and REES, 1970; HROUDA, 1982; TARLING and HROUDA, 1993) were used in this study. In detail, a sample that had a foliated ellipsoid with  $q$  values less than 0.7 and  $K_3$  directions lying within 25° of the vertical was con-

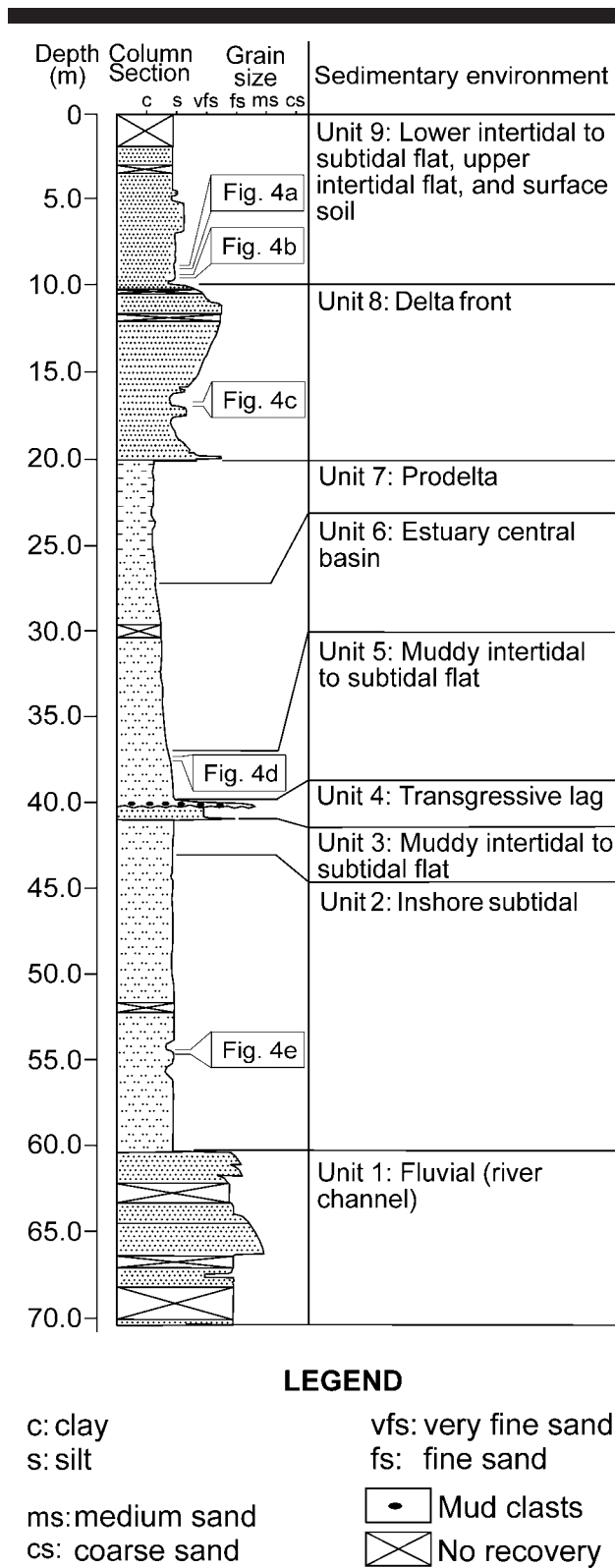


Figure 2. Column section of borehole CM-97. The section was divided into nine stratigraphic units; the sedimentary facies are shown on the right. Also shown are the locations of the horizons (shown in Figure 4a-e) that are used in the discussion of the sedimentary structures and AMS paleocurrents.

sidered primary magnetic fabric and used in paleocurrent determination.

The natural remanent magnetization (NRM) was then measured and demagnetized using a three-axis 2G Enterprises cryogenic magnetometer with an inline alternating field (AF) demagnetizer with a peak field strength of 80 mT. First, all odd-numbered samples were subjected to incremental AF demagnetization at steps of 0, 5, 10, 15, 20, 25, 30, 35, 40, 50, 60, and 80 mT. Because the statistical and visual analysis of this detailed demagnetization spectrum showed that most samples exhibited sufficient stability, we decided to treat the remaining samples (the even-numbered samples) at steps of 0, 20, 30, and 40 mT. Figure 3 shows typical examples of the demagnetization behaviors obtained. Combined visual (using stereographic and orthogonal plots) and statistical (using the principal component analysis of KIRSCHVINK, 1980) inspections of demagnetization data indicated that 20 mT AF demagnetization was sufficient to remove viscous remanence and isolate the stable relative magnetic north direction for most samples. The relative magnetic north direction at each sample level was then calculated from a linear fitting of declinations obtained at 20 mT with depth and used for reorientation of the AMS directions to their geographic coordinates to obtain absolute paleocurrent directions (ABDELDAYEM *et al.*, 1999).

Primary sedimentary structures (cross-laminations) were described on the basis of detailed examination of X-ray photographs of the subcores. Paleocurrents were first inferred from the dip of these primary foreset laminae and then from the *in situ* AMS data. Paleocurrent directions from both the sedimentary structures and the *in situ* AMS data were based on the core coordinate system; *i.e.*, paleocurrent directions are to the left or right relative to the subcore section. By doing so, we assumed that the subcore section was cut in the east-west direction and that the AMS sample box was pressed into the surface facing south; thus, downhole paleocurrent directions  $-90$  and  $90$  determined from the *in situ* AMS data corresponded to left and right inferred from the primary cross-laminations, respectively. Therefore, the current direction results, from both the primary cross-laminations and the *in situ* AMS data, were in the same coordinate system and thus were comparable.

Lower hemisphere equal-area projections of  $K_1$  and  $K_3$  were also done on some samples using the reoriented AMS data to obtain absolute paleocurrent directions.

## RESULTS AND ANALYSIS

### Sedimentary Structural Features

Sedimentary structures, especially cross-laminations with clear foresets, can tell us the direction of the current when the sediments were deposited (ALLEN, 1984; READING, 1996; REINECK and SINGH, 1980). Based on the detailed examination of the X-ray photographs of the subcores, primary sedimentary structures with clear cross-lamination were found in 19 of 35 subcores, among which five subcores (A6, A7, B17, B30, and B38) had bidirectional cross-laminations (Table 1), showing that there were bidirectional flows, *i.e.*, tidal currents. Primary cross-laminations were found in 35 horizons,

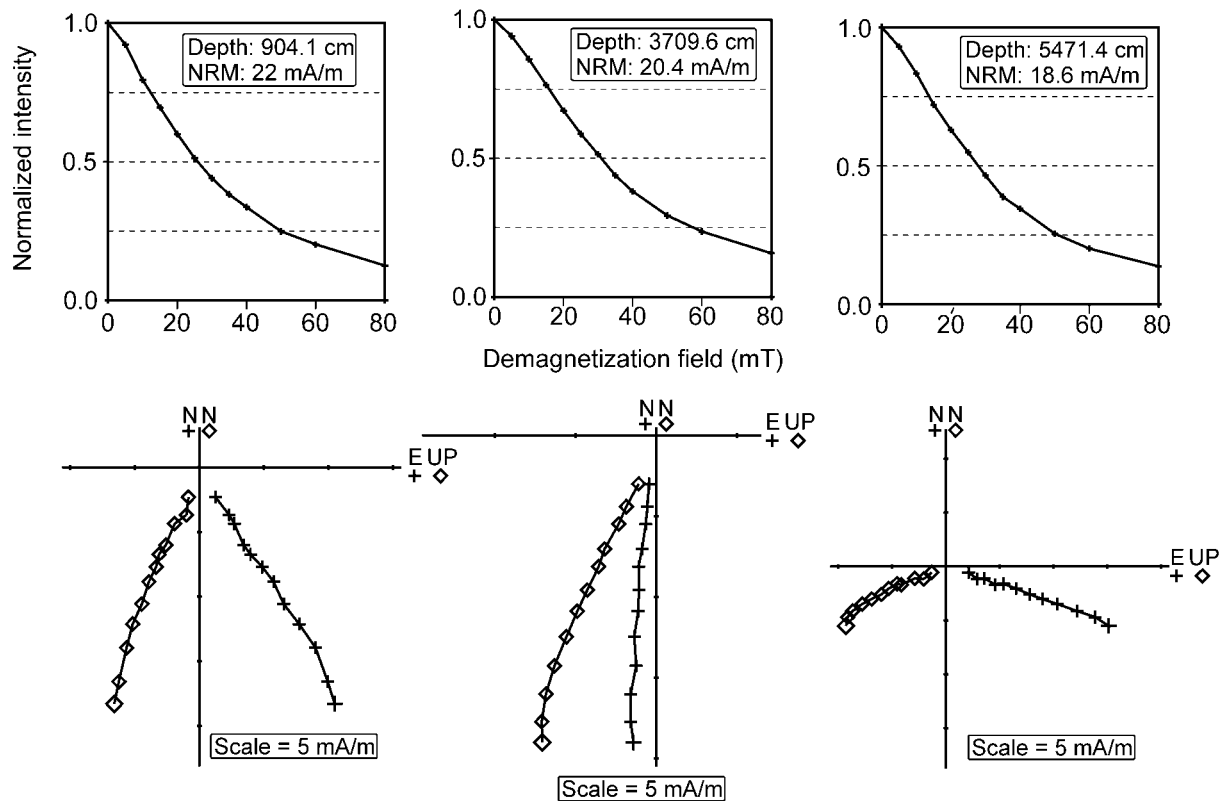


Figure 3. Typical examples of direction and intensity changes during AF demagnetization of samples from borehole CM-97. Upper: Normalized NRM intensity versus AF peak amplitudes. Sample depth and NRM of each sample are shown in the plots. Lower: Orthogonal projections (Zijderveld diagrams; ZIJDERVELD, 1976) of the stepwise demagnetization of the same samples. Units of each sample are shown in the plots. The NRM measurement for each sample is marked with a larger symbol. Horizontal projections are marked with plus signs and vertical projections are marked with open squares. It is clear that 20 mT of AF is enough to remove viscous remanence and isolate the stable relative magnetic north directions.

whose thickness ranged from 3 to 12 mm with an average of 7.7 mm (Table 1), with foreset laminae dipped to the left or right relative to the corresponding subcore section (Table 1), indicating current direction to the left or right, respectively. In general, the primary sedimentary structures showed bidirectional flow characteristics in these sediments.

#### Comparative Study of Paleocurrent Directions Obtained From the Sedimentary Structures and the *In Situ* AMS Data

To probe the AMS characteristics of tide-influenced sediments, we conducted detailed comparisons between the paleocurrent results obtained from the primary sedimentary structures and those indicated by the *in situ* AMS data, based on the subcores with bidirectional cross-laminations.

In subcore A7, primary cross-laminations were found in five horizons (Table 1, Figure 4a, 4b). Lamination A was located between 8.922 and 8.930 m depth and had a thickness of 8 mm and an apparent dip angle of 15°; it dipped to the left, indicating a paleocurrent direction to the left, and the corresponding paleocurrent direction estimated from the *in situ* AMS data was also to the left (Table 1, Figure 4a). Lamination B was located at 8.972 to 8.977 m depth and had a

thickness of 5 mm and an apparent dip angle of 15°; it also dipped to the left, indicating a paleocurrent direction to the left, and the corresponding paleocurrent direction from the *in situ* AMS data was also to the left (Table 1, Figure 4a). Lamination C was located at 8.988 to 8.993 m depth, with a thickness of 5 mm and an apparent dip angle of 15°; it dipped to the left, indicating a paleocurrent direction to the left, while the corresponding AMS paleocurrent direction was to the right (Table 1, Figure 4a). Lamination D was located at 9.657 to 9.664 m depth, with a thickness of 7 mm and an apparent dip angle of 10–15°; it dipped to the left, indicating a paleocurrent direction to the left (Table 1, Figure 4b). This horizon did not correspond to one single AMS sample (Figure 4b). Lamination E, located at 9.675 to 9.686 m depth, with a thickness of 11 mm and an apparent dip angle of 20°, dipped to the right, indicating a paleocurrent direction to the right, and the corresponding AMS paleocurrent direction was also to the right (Table 1, Figure 4b).

Among the paleocurrent directions determined from the five cross-laminations in subcore A7 (Figure 4a, 4b, Table 1), A, B, and E are in good accordance with those indicated by the *in situ* AMS data (Figure 4a, 4b), while C is opposite to that estimated by the *in situ* AMS data (Figure 4a), and D is

Table 1. Primary sedimentary structures and paleocurrents relative to core section. The cross-lamination description is based on detailed examination of X-ray photos. Paleocurrent directions are inferred from the dip of the foreset laminae. Note that cores A6, A7, B17, B30, and B38 had bidirectional cross-laminations. The letters A, B, C, . . . , N on the right side correspond to the cross-laminations on Figures 4a–e.

Subcore			Foreset Description				
Core No.	Depth (m)	Thickness (m)	Horizon (m)	Thickness (mm)	Direction and Apparent Angle (°) of Dip	Paleocurrent Direction	
A3	3.70–4.45	0.75	3.869–3.872	3	Right, 10	Right	
A4	4.60–5.90	1.30	5.373–5.380	7	Left, 15	Left	
A5	5.95–7.35	1.40	7.230–7.240	10	Right, 10	Right	
A6	7.40–8.80	1.40	8.035–8.045	10	Left, 30	Left	
A7	8.85–10.25	1.40	8.172–8.180	8	Right, 20	Right	
			8.253–8.261	8	Left, 30	Left	
			8.922–8.930	8	left, 15	Left	A
			8.972–8.977	5	Left, 15	Left	B
			8.988–8.993	5	Left, 15	Left	C
			9.657–9.664	7	Left, 10–15	Left	D
B15	12.90–14.30	1.40	9.675–9.686	11	Right, 20	Right	E
			13.430–13.436	6	Left, 20	Left	
B16	14.80–15.75	0.95	15.725–15.735	10	Left, 10	Left	
B17	15.80–17.20	1.40	16.350–16.360	10	Right, 15	Right	F
			16.374–16.386	12	Right, 15	Right	G
			16.394–16.400	6	Left, 5	Left	H
B25	27.55–29.60	2.05	28.203–28.210	7	Left, 30	Left	
			28.220–28.232	12	Left, 30	Left	
B27	30.38–31.85	1.47	30.723–30.730	7	Right, 5	Right	
B29	34.35–36.50	2.15	35.490–35.499	9	Left, 25	Left	
B30	36.80–38.75	1.95	36.860–36.864	4	Right, 15	Right	
			37.068–37.071	3	Right, 10	Right	I
			37.073–37.080	7	Left, 30	Left	J
			37.770–37.780	10	Left, 20	Left	
B31	38.80–40.95	2.15	38.884–38.891	7	Left, 10	Left	
			39.156–39.162	6	Left, 20	Left	
			44.388–44.397	9	Right, 10	Right	
B33	43.30–45.45	2.15	44.388–44.397	9	Right, 10	Right	
B34	45.55–47.70	2.15	45.593–45.598	5	Right, 10	Right	
B35	47.80–49.95	2.15	49.370–49.380	10	Left, 20	Left	
B37	52.27–54.40	2.13	52.540–52.551	11	Right, 20	Right	
B38	54.50–56.65	2.15	54.698–54.702	5	Left, 10	Left	K
			54.714–54.723	8	Left, 20	Left	L
			54.757–54.765	8	Right, 20	Right	M
			54.771–54.785	14	Left, 19	Left	N
B39	56.75–58.50	1.75	57.378–57.386	8	Right, 20	Right	

not clear because it might have been divided into two AMS samples (Figure 4b). Besides the sedimentary structures, the *in situ* AMS data also showed bidirectional flow features (Figure 4a, 4b). However, no absolute paleocurrent directions could be inferred for these sediments because the reoriented  $K_3$  scattered around the center on the lower-hemisphere equal-area projections of  $K_1$  and  $K_3$ , without clear imbrication (Figure 4a, 4b).

In subcore B17, cross-laminations were found at three horizons (Table 1, Figure 4c). Lamination F, located at 16.350 to 16.360 m depth, with a thickness of 10 mm and an apparent dip angle of 15°, dipped to the right, indicating a paleocurrent direction to the right, and the corresponding AMS paleocurrent direction was also to the right (Table 1, Figure 4c). Lamination G, 16.374 to 16.386 m deep, 12 mm thick, and an apparent dip angle 15° to the right, indicated a paleocurrent direction to the right, with the corresponding AMS paleocurrent direction also to the right (Table 1, Figure 4c). Lamination H, 16.394 to 16.400 m deep, 6 mm tick, and an apparent dip angle of 5° to the left, indicated a paleocurrent

direction to the left, but the corresponding AMS paleocurrent direction was to the right (Table 1, Figure 4c). Among the paleocurrent directions determined from these three cross-laminations, F and G were in good accordance with those estimated from the *in situ* AMS data (Figure 4c), while H was not. The *in situ* AMS data did not show bidirectional flow features even though the sedimentary structures showed bidirectional flows (Figure 4c).

In subcore B30, cross-laminations were found at four horizons (Table 1). We selected the interval from 37.00 to 37.25 m depth for detailed comparison (Figure 4d). Lamination I, at 37.068 to 37.071 m depth, was 3 mm thick and had an apparent dip angle of 10° to the right, indicating a paleocurrent direction to the right, but the corresponding AMS paleocurrent direction was to the left (Table 1, Figure 4d). Lamination J, 37.073 to 37.080 m deep, 7 mm thick, and an apparent dip angle of 30° to the left, indicated that a paleocurrent direction was to the left, and the corresponding AMS paleocurrent direction was also to the left (Table 1, Figure 4d). The paleocurrent determined from lamination J was in

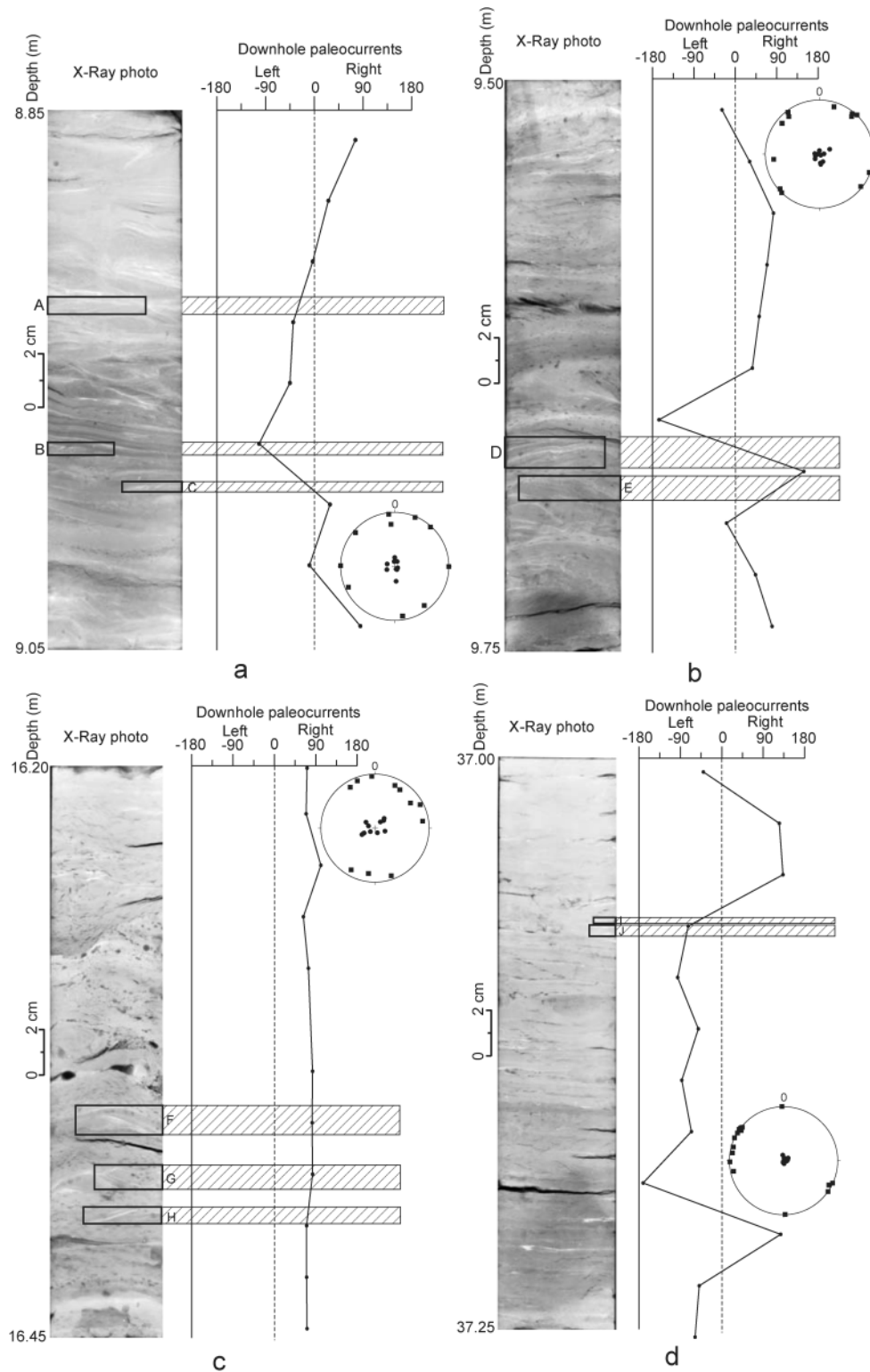


Figure 4. Comparison between paleocurrents determined from the sedimentary structures and those indicated by the *in situ* AMS data. (a) The section 8.85 to 9.05 m deep in subcore A7. (b) The section 9.50 to 9.75 m deep in subcore A7. (c) The section 16.20 to 16.45 m deep in subcore B17. (d) The section 37.00 to 37.25 m deep in subcore B30. (e) The section 54.65 to 54.85 m deep in subcore B38. On the left is the X-ray photo image, while on the right is the downhole paleocurrent as determined from the *in situ* AMS data ( $D_1$ ). Primary cross-laminations are marked with rectangles on the X-ray photos and the paleocurrents inferred are shown with open arrows pointing in the flow direction. For the downhole paleocurrents determined from the *in situ* AMS data,  $-90$  represents left, while  $90$  represents right. The cross-laminations A, B, E, F, G, J, K, L, and N are in good accordance with the *in situ* AMS data. Lower-hemisphere equal-area stereographic projections of the reoriented  $K_1$  (solid square) and  $K_3$  (solid circle) of these samples are also shown in the plot.

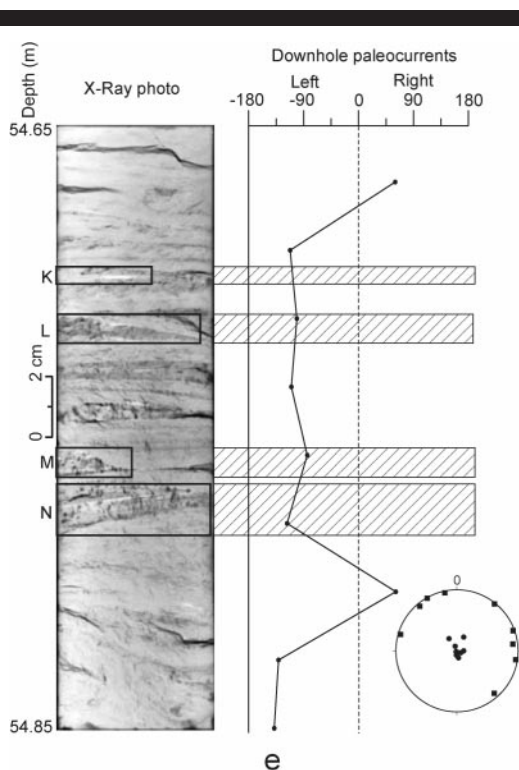


Figure 4. Continued.

good accordance with that estimated by the *in situ* AMS data, but the same was not true for lamination I (Figure 4d). However, it is clear that both laminations I and J were collected as one AMS sample, not two separate samples (Figure 4d), and lamination I was much thinner than J. Like the sedimentary structures, the *in situ* AMS data also showed bidirectional flow features clearly (Figure 4d). From the lower-hemisphere equal-area projections of reoriented  $K_1$  and  $K_3$ , the paleocurrent direction seems to have been northwest to southeast, but no absolute direction could be inferred because there was no clear imbrication of  $K_3$  (Figure 4d).

In subcore B38, cross-laminations were found at four horizons (Table 1, Figure 4e). Lamination K was located at 54.698 to 54.702 m depth, with a thickness of 5 mm and an apparent dip angle of  $10^\circ$  to the left, indicating a paleocurrent direction to the left, and the corresponding AMS paleocurrent direction was also to the left (Table 1, Figure 4e). Lamination L, 54.714 to 54.723 m deep, 8 mm thick, and an apparent dip angle of  $20^\circ$  to the left, indicated a paleocurrent direction to the left, with the corresponding AMS paleocurrent direction also to the left (Table 1, Figure 4e). Lamination M, located at 54.757 to 54.765 m depth, with a thickness of 8 mm and an apparent dip angle of  $20^\circ$  to the right, indicated a paleocurrent direction to the right, but the corresponding AMS paleocurrent direction was to the left (Table 1, Figure 4e). Lamination N was located between 54.771 and 54.785 m depth and had a thickness of 14 mm and an apparent dip angle of  $19^\circ$  to the left, indicating a paleocurrent direction to the left, and the corresponding AMS paleocurrent direction

was also to the left (Table 1, Figure 4e). Paleocurrents determined from the cross-laminations K, L, and N were in good accordance with those indicated by the *in situ* AMS data; all were to the left, but lamination M indicated a current direction opposite to that indicated by the *in situ* AMS data (Figure 4e). Both the sedimentary structures and AMS showed bidirectional flow features in these sediments (Figure 4e).

In general, not only the primary sedimentary structures but also the *in situ* AMS data showed bidirectional flow characteristics in these sediments. Among 14 cross-laminations discussed previously, nine (about 64.3%) showed the same paleocurrent direction (either to the right or to the left as that indicated by the *in situ* AMS data).

### Downhole Paleocurrent Changes from the *In Situ* AMS Data

Borehole CM-97 was divided into nine stratigraphic units (HORI *et al.*, 1999), of which unit 5 was deposited in a muddy intertidal- to subtidal-flat environment, unit 6 consisted of Changjiang estuary central basin sediments, and unit 8 comprised delta front sediments (HORI *et al.*, 2001a, 2001b). We used the *in situ* declination ( $D_1$ ) of maximum susceptibility ( $K_1$ ) to obtain downhole paleocurrent changes for the whole core section of these three stratigraphic units (Figure 5a, 5b, 5c).

The muddy intertidal- to subtidal-flat sediments, downhole paleocurrent changes showed bidirectional processes very clearly (Figure 5a). Based on downhole paleocurrent features, this unit was subdivided into three parts: in the upper part (36.80–37.87 m depth), there were regular bidirectional flows; the middle part (37.87–39.20 m depth) was dominated by right-directed unidirectional flow; and the lower part (39.20–39.80 m depth) also showed bidirectional flow features, with about two-thirds of the flows directed to the right (Figure 5a). Absolute paleocurrent directions determined from lower-hemisphere equal-area stereographic projections of reoriented  $K_1$  and  $K_3$  for samples from the upper part of the unit also indicated clear bidirectional flow features, shown by open arrows, with  $K_3$  of the samples imbricated to the northwest and southeast (Figure 5a).

The Changjiang estuary central basin sediments also showed bidirectional flow features, although they were quite different from those of the muddy intertidal- to subtidal-flat sediments (Figure 5a, 5b). These downhole paleocurrents were not as regular as those of the intertidal- to subtidal-flat sediments, but the whole stratigraphic unit resembled the lower part of unit 5, *i.e.*, bidirectional currents with right-directed flows dominant.

Similarly, the delta front sediments also showed prevailing current direction to the right, although some samples indicated a left-directed current (Figure 5c). Compared with the Changjiang estuary central basin sediments, the delta front sediments seemed to be controlled to a greater degree by a unidirectional current.

These differences between the downhole paleocurrent features of units 5, 6, and 8 may reflect hydrodynamic differences among these three sedimentary environments.

In general, downhole paleocurrent changes in all the inter-

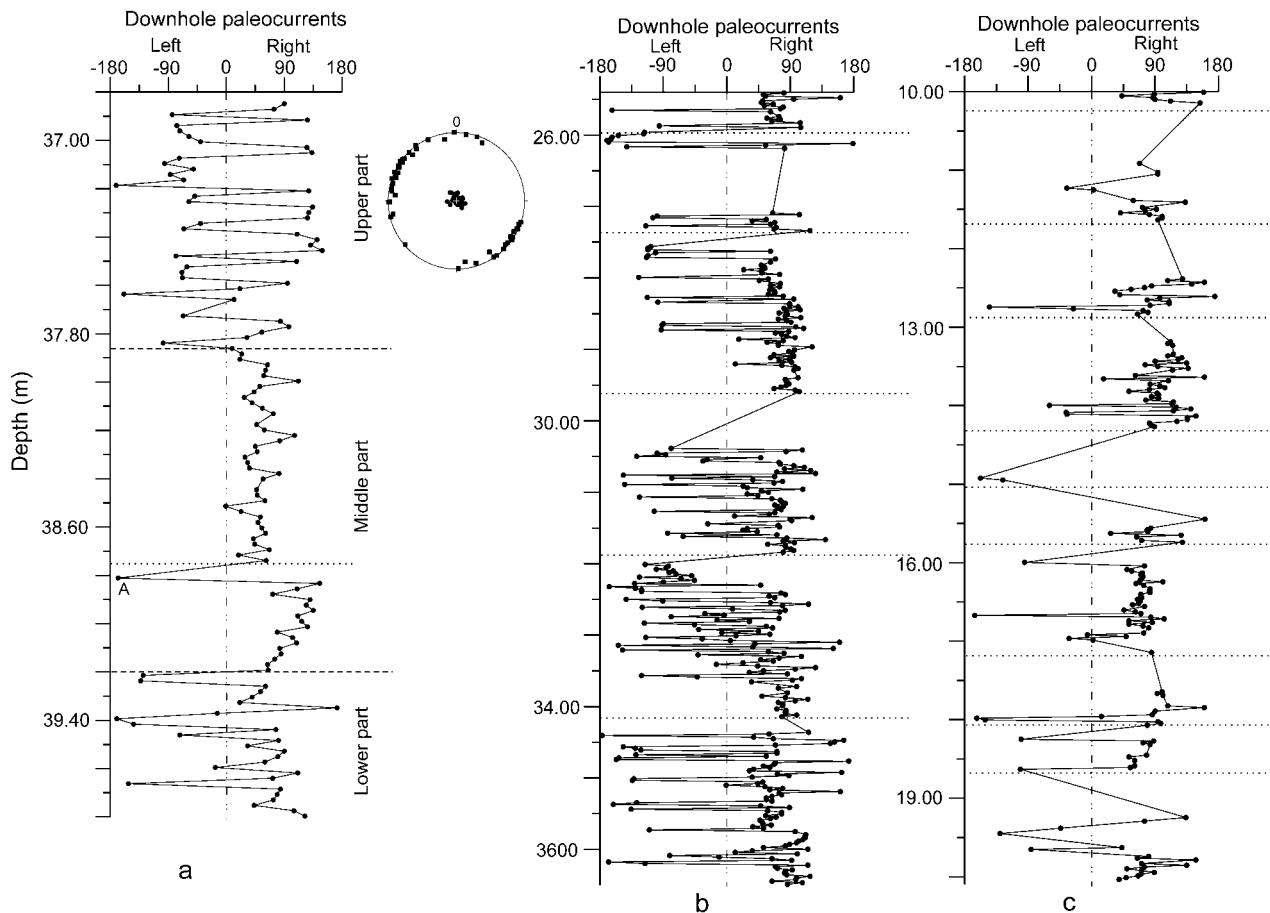


Figure 5. Downhole paleocurrent changes. (a) Muddy intertidal to subtidal sediments. (b) Changjiang estuary central basin sediments. (c) Delta front sediments. The downhole paleocurrents were inferred from the *in situ* declination ( $D_1$ ) of maximum susceptibility ( $K_1$ ). Left is represented by  $-90$ , while right is represented by  $90$ . The downhole paleocurrent features clearly show the bidirectional flows, indicating tidal processes, especially for the muddy intertidal to subtidal sediments. Unit 5 strata were subdivided into upper, middle, and lower parts, with the boundaries marked by dashed lines. The dotted lines show the boundary between two subcores. Lower-hemisphere equal-area stereographic projections of the reoriented  $K_1$  (solid square) and  $K_3$  (solid circle) of the samples from the upper part of unit 5 also show bidirectional flow features (open arrows).

tidal- to subtidal-flat, Changjiang estuary central basin, and delta front sediments showed bidirectional flow features, even though there were differences among them.

### AMS Characteristics of These Tide-Influenced CM-97 Sediments

We use unit 5 as an example to discuss the AMS characteristics of CM-97 tide-influenced sediments. As mentioned previously, sediments of this unit were deposited in an intertidal- to subtidal-flat environment (HORI *et al.*, 2001a, 2001b). Figure 6 shows the downhole changes in mean magnetic susceptibility ( $K$ ), corrected anisotropy degree ( $P_j$ ), magnetic lineation ( $L$ ), magnetic foliation ( $F$ ), and the shape parameter ( $q$ ) of unit 5.

There were obvious downhole changes in mean susceptibility ( $K$ ), which averaged  $492.1 \times 10^{-6}$  SI, with a minimum of  $374.6 \times 10^{-6}$  SI and a maximum of  $831.9 \times 10^{-6}$  SI (Figure 6). There were also obvious downhole changes in the correct-

ed anisotropy degree ( $P_j$ ), which averaged 1.112, with a minimum of 1.047 and a maximum of 1.157 (Figure 6). The downhole changes in  $L$ ,  $F$ , and  $q$  were different from those in  $K$  and  $P_j$ , with only the changes in the middle part of the unit like those of  $K$  and  $P_j$ , while the upper and lower parts were without obvious downhole changes (Figure 6). The average, minimum, and maximum values were, respectively, 1.011, 1.001, and 1.062 for  $L$ ; 1.089, 1.030, and 1.129 for  $F$ ; and 0.123, 0.006, and 0.615 for  $q$ .

Unit 5 can also be subdivided into three parts based on the downhole changes in  $K$ ,  $P_j$ ,  $L$ ,  $F$ , and  $q$  (Figure 6). The upper part (36.80–37.63 m depth) had no obvious downhole changes in  $L$ ,  $F$ , or  $q$ , although there were obvious downhole changes in  $K$  and  $P_j$ ; the middle part (37.63–38.80 m depth) had obvious downhole changes in all the parameters  $K$ ,  $P_j$ ,  $L$ ,  $F$ , and  $q$ ; and the lower part (38.80–39.80 m depth) had no obvious downhole changes in  $L$ ,  $F$ , or  $q$ , although there were obvious downhole changes in  $K$  and  $P_j$ , except near the bottom, where  $F$  and  $q$  also changed obviously.

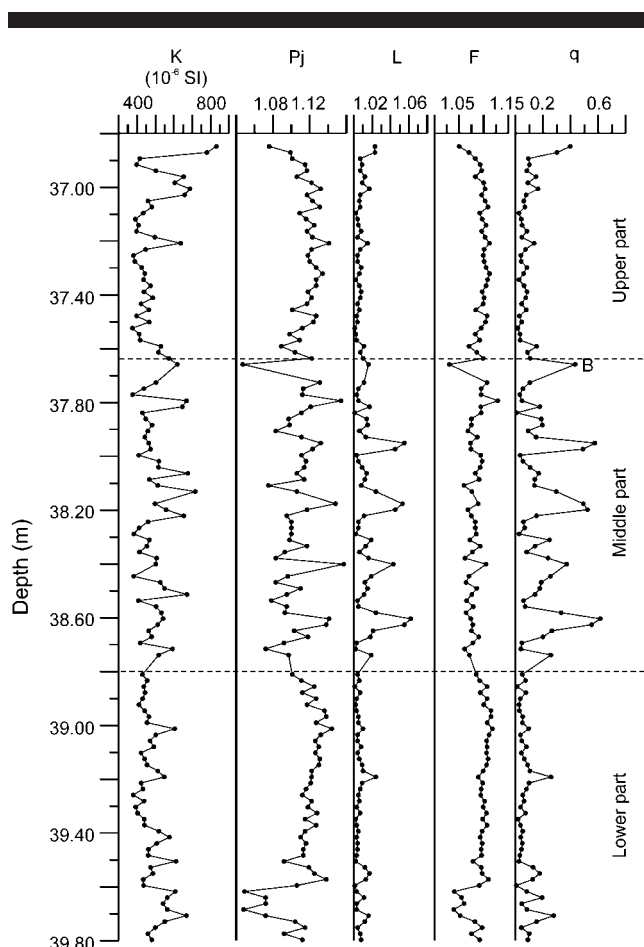


Figure 6. Anisotropy of magnetic susceptibility characteristics of stratigraphic unit 5. Downhole changes in mean magnetic susceptibility ( $K$ ), corrected anisotropy degree ( $P_j$ ), magnetic lineation ( $L$ ), magnetic foliation ( $F$ ), and the shape parameter ( $q$ ) are shown in this figure. The strata were subdivided into upper, middle, and lower parts based on downhole changes in these parameters, with the boundaries marked by dashed lines.

## DISCUSSION

Primary sedimentary structures (cross-laminations) were found in 35 horizons of the subcore section of borehole CM-97 with the tide-influenced estuary or delta sediments. These cross-laminations enabled us to determine current directions during their formation. The bidirectional flow features, especially in the five subcores with bidirectional cross-laminations, indicated that these sediments were deposited by tidal currents. Furthermore, absolute paleocurrent directions ascertained from the reoriented AMS data from the upper part of unit 5 also showed bidirectional flow features, with the currents directed northwest and southeast. The directions are in good accordance with the tidal features in this area (LI and WANG, 1998). Unfortunately, we could not compare the cross-laminations among different subcores because they do not have the same cut direction when the subcores were split into two halves. Otherwise, we might have been able to find more bidirectional sedimentary structures.

Other sedimentary structures, such as sand-mud couplets, representing daily tidal cycles and neap-spring tide cycles, have also been found in the CM-97 samples (HORI *et al.*, 2001a, 2001b). In fact, sedimentary structures formed under tidal processes have been widely found in the Changjiang delta estuarine and deltaic sediments (LI *et al.*, 2000, 2001). Therefore, these sediments were deposited in a strong tide-influenced environment.

Comparison of the paleocurrents determined from the sedimentary structures and those indicated by the *in situ* AMS data showed that more than 64% were in agreement with respect to current direction. In the case of the other five cross-laminations that indicated different current directions from those indicated by the *in situ* AMS data, the differences in AMS sample size relative to the thickness of the cross-lamination may explain the discrepancy. In other words, many of the cross-laminations were too thin to be able to control the mean flow direction of the whole AMS sample in which they were located. More than 68% of the cross-laminations were less than 10 mm thick, which is much smaller than the thickness of a single AMS sample (20 mm). A cross-lamination can show the current direction of its horizon, while AMS data can only indicate the mean current direction for the whole 20-mm-thick stratum. We could infer the current direction from the cross-laminations found, but we could not determine the current direction of the other sediments for which no cross-laminations were available and whose current directions might or might not be the same as that of the part with the cross-lamination. In addition, some cross-laminations, such as lamination D, might have been cut into two parts and divided into two samples (Figure 4b). On the other hand, two thin cross-laminations, such as laminations I and J, also might have been included in one sample (Figure 4d). Since J is much thicker than I, it may have counteracted the effect of I. These possibilities could result in the AMS data indicating a mean direction different from that indicated by a cross-lamination located in the same horizon.

The characteristics of downhole paleocurrent changes differed among the muddy intertidal- to subtidal-flat, estuary central basin, and delta front sediments, perhaps because of hydrodynamic differences among these three sedimentary environments. Hydrodynamic conditions in the intertidal- to subtidal-flat environment are controlled by typical bidirectional flood and ebb tidal currents, with the speed of flood tidal currents generally greater than that of ebb tidal currents (KLEIN, 1985). Hydrodynamic conditions of the estuary and delta front environments are comprehensively influenced by river flow, tidal currents, waves and wind, and other factors (NICHOLS and BIGGS, 1985; WRIGHT, 1985). These hydrodynamic factors affect AMS, *i.e.*, the alignment of magnetic minerals.

Sedimentary paleoenvironments since the Late Pleistocene in the Changjiang estuary have been found to be controlled by flood-tidal currents (LIU *et al.*, 2001), and tidal currents have been inferred to have been much stronger during the Holocene transgression than at present (LI *et al.*, 2002), which may be why downhole paleocurrent changes in the Changjiang estuary central basin and delta front sediments were dominated by unidirectional flow features.

Magnetic susceptibility has been found very useful for stratigraphic division and correlation (ARAI *et al.*, 1997; BARTHÈS *et al.*, 1999; CRICK *et al.*, 1997; ELLWOOD *et al.*, 1999; HELLER and LIU, 1982). Furthermore, downhole changes in  $K$ ,  $P_j$ ,  $L$ ,  $F$ , and  $q$  have been found corresponding well to the nine stratigraphic units of CM-97 (LIU *et al.*, 2001). In the present study we found that unit 5 could be subdivided into three parts on the basis of both downhole paleocurrents and downhole changes in AMS parameters (Figures 5a, 6). When we examined changes in downhole AMS parameters carefully, we found that the boundary mismatch might be due to a single sample, *e.g.*, the sample marked "B" near the boundary between the upper and middle parts of Unit 5 (Figure 6). Without sample B, the boundary could be put at 37.87 m depth, which is exactly the same depth as the boundary indicated by the downhole paleocurrent changes. Similarly, the boundary between the middle and lower parts of unit 5 based on changes in downhole AMS parameters corresponded to the sample marked "A" on the graph showing downhole paleocurrent changes (Figure 5a). It would be better to put the boundary between the middle and lower parts of the unit at 38.80 m depth because it is clear that the downhole paleocurrent directions for the strata between 38.80 and 39.20 m depth differed from those above 38.80 m depth even though they were also right directed (Figure 5a), and the differences above and below 38.80 m deep were quite clear with respect to the changes in downhole AMS parameters (Figure 6).

### CONCLUSIONS

Primary sedimentary structures (cross-laminations) were observed in 35 horizons distributed on 19 of 35 subcores, among which five subcores had bidirectional cross-laminations, showing that these sediments were deposited by bidirectional currents. More than 64% of the cross-laminations found on the five subcores with bidirectional flow features indicated paleocurrent directions matching those inferred from the *in situ* AMS data, even though more than 68% of the cross-laminations were thinner than 10 mm, half thickness of the AMS samples, demonstrating that AMS data can supply us with true paleocurrent directions for coastal tidal-influenced estuary or delta sediments. Downhole paleocurrent changes determined from the *in situ* AMS data also showed bidirectional flow features of the intertidal to subtidal flat, Changjiang estuary central basin, and delta front sediments, although the features indicating the changes differed in detail. These differences in the downhole paleocurrent changes of sediments deposited in different sedimentary paleoenvironments may have resulted from differences in the hydrodynamic conditions of the specific environment.

AMS characteristics of tide-influenced sediments from borehole core CM-97 clearly showed the possibility of subdividing strata in detail. The strata of stratigraphic unit 5 were subdivided into three parts, showing that AMS may be useful for determining stratigraphic divisions and for detailed reconstruction of sedimentary paleoenvironments.

### ACKNOWLEDGMENTS

The authors are grateful to Professors Pinxian Wang and Xinrong Chen and the staff of Marine Geology Laboratory at

Tongji University, Shanghai, China, for their great help during the coring and subsampling. This research is funded by the Global Environment Research Fund of the Environment Agency of Japan. B. Liu would like to express his special thanks to STA/JST/JISTEC of Japan for making it possible for him to conduct this study under an STA Fellowship and Dr. Gregory Stone at Coastal Studies Institute, Louisiana State University for his help and encouragement in preparing the manuscript. We thank the two reviewers for their time and effort in helping us prepare this paper for publication.

### LITERATURE CITED

- ABDELDAYEM, A.L.; YAMAZAKI, T., and IKEHARA, K., 1999. MAGNETIC SUSCEPTIBILITY ANISOTROPY AND REMANENCE OF SOME DEEP-SEA SEDIMENTS OF THE TOKAI BASIN. In: YUASA, M., (ed.), *Marine Geological Investigations of the Tokai Offshore Area, Tsukuba, Japan: Geological Survey of Japan*, pp. 127–146.
- ALLEN, J.R.L., 1984. *Sedimentary Structures—their Character and Physical Basis*. Amsterdam: Elsevier.
- ARAI, K.; SAKAI, H., and KONISHI, K., 1997. High-resolution rock-magnetic variability in shallow marine sediment: a sensitive paleoclimatic metronome. *Sedimentary Geology*, 110, 7–23.
- BALSLEY, J.R. and BUDDINGTON, A.F., 1960. Magnetic susceptibility anisotropy and fabric of some Adirondack granites and orthogneisses. *American Journal of Science*, 258, 6–20.
- BARTHÈS, V.; POZZI, J.P.; VIBERT-CHARBONNEL, P.; THIBAL, J., and MÉLIÈRES, M.A., 1999. High-resolution chronostratigraphy from downhole susceptibility logging tuned by palaeoclimatic orbital frequencies. *Earth and Planetary Science Letters*, 165, 97–116.
- CRICK, R.E.; ELLWOOD, B.B.; EL HASSANI, A.; FEIST, R., and HLADIL, J., 1997. Magnetosusceptibility event and cyclostratigraphy (MSEC) of the Eifelian-Givetian GSSP and associated boundary sequences in North Africa and Europe. *Episodes*, 20, 167–175.
- ELLWOOD, B.B., 1980. Application of the anisotropy of magnetic susceptibility method as an indicator of bottom-water flow direction. *Marine Geology*, 34, M83–M90.
- ELLWOOD, B.B., 1984. Bioturbation: minimal effects on the magnetic fabric of some natural and experimental sediments. *Earth and Planetary Science Letters*, 67, 367–376.
- ELLWOOD, B.B. and LEDBETTER, M.T., 1977. Antarctic bottom water fluctuations in the Vema Channel: effects of velocity changes on particle alignment and size. *Earth and Planetary Science Letters*, 35, 189–198.
- ELLWOOD, B.B. and LEDBETTER, M.T., 1979. Paleocurrent indicators in deep-sea sediment. *Science*, 203, 1335–1337.
- ELLWOOD, B.B.; LEDBETTER, M.T., and JOHNSON, D.A., 1979. Sedimentary fabric: a tool to delineate a high-velocity zone within a deep western Indian Ocean bottom current. *Marine Geology*, 33, M51–M55.
- ELLWOOD, B.B.; HROUDA, F., and WAGNER, J., 1988. Symposia on magnetic fabrics: introductory comments. *Physics of the Earth and Planetary Interiors*, 51, 249–252.
- ELLWOOD, B.B.; CRICK, R.E., and EL HASSANI, A., 1999. The magneto-susceptibility event and cyclostratigraphy (MSEC) method used in geological correlation of Devonian rocks from Anti-Atlas Morocco. *AAPG Bulletin*, 83, 1119–1134.
- GRANAR, L., 1958. Magnetic measurements on Swedish varved sediments. *Arkiv för Geofysik*, 3, 1–40.
- HAMILTON, N. and REES, A.I., 1970. The use of magnetic fabric in palaeocurrent estimation. In: RUNCORN, S.K. (ed.), *Palaeogeophysics*. London: Academic Press, pp. 445–464.
- HELLER, F. and LIU, T.S., 1982. Magnetostatigraphical dating of loess deposits in China. *Nature*, 300, 431–433.
- HORI, K.; SAITO, Y.; ZHAO, Q.; CHENG, X.; WANG, P., and LI, C., 1999. Sedimentary characteristics of post-glacial deposits beneath the Changjiang River delta. In: SAITO, Y., *et al.* (eds.), *Proceedings of an International Workshop on Sediment Transport and Storage*

- in *Coastal Sea-Ocean System*. Tsukuba, Japan, March 15–19, 1999, pp. 39–43.
- HORI, K.; SAITO, Y.; ZHAO, Q.; CHENG, X.; WANG, P.; SATO, Y., and LI, C., 2001a. Sedimentary facies and Holocene progradation rates of the Changjiang (Yangtze) delta, China. *Geomorphology*, 41, 233–248.
- HORI, K.; SAITO, Y.; ZHAO, Q.; CHENG, X.; WANG, P.; SATO, Y., and LI, C., 2001b. Sedimentary facies of the tide-dominated paleo-Changjiang (Yangtze) estuary during the last transgression. *Marine Geology*, 177, 331–351.
- HROUDA, F., 1982. Magnetic anisotropy of rocks and its application in geology and geophysics. *Geophysical Surveys*, 5, 37–82.
- ISING, G., 1942. On the magnetic properties of varved clay. *Ark. Mat. Arkiv för Matematik Astronomi och Fysik*, 29, 1–37.
- JELINEK, V., 1981. Characterization of the magnetic fabric of rocks. *Tectonophysics*, 79, T63–T67.
- KIRSCHVINK, J.L., 1980. The least-squares line and plane and the analysis of palaeomagnetic data. *Geophysical Journal of the Royal Astronomical Society*, 62, 699–718.
- KLEIN, G., 1985. Intertidal flats and intertidal sand bodies. In: DAVIS, R.A., JR. (ed.), *Coastal Sedimentary Environments*. 2nd revised, expanded edition. New York: Springer-Verlag, pp. 187–224.
- LAGROIX, F. and BANERJEE, S.K., 2002. Paleowind directions from the magnetic fabric of loess profiles in central Alaska. *Earth and Planetary Science Letters*, 195, 99–112.
- LEDBETTER, M.T. and ELLWOOD, B.B., 1980. Spatial and temporal changes in bottom-water velocity and direction from analysis of particle size and alignment in deep-sea sediment. *Marine Geology*, 38, 245–261.
- LI, C. and WANG, P., 1998. *Late Quaternary Stratigraphy of the Changjiang Delta*. Beijing: China Science Press. (in Chinese)
- LI, C.; CHEN, Q.; ZHANG, J.; YANG, S., and FAN, D., 2000. Stratigraphy and paleoenvironmental changes in the Yangtze Delta during the Late Quaternary. *Journal of Asian Earth Sciences*, 18, 453–469.
- LI, C.; FAN, D.; HORI, K.; ZHAO, Q.; SAITO, Y., and CHENG, X., 2000. Some problems on postglacial transgression-regression and environmental evolution in the Changjiang delta. *Journal of Nanjing Normal University*, 23(4), 181–188. (in Chinese, with English abstract)
- LIU, B.; SAITO, Y.; YAMAZAKI, T.; ABDELDAYEM, A.; ODA, H.; HORI, K., and ZHAO, Q., 2001. Paleocurrent analysis for the Late Pleistocene-Holocene incised-valley fill of the Yangtze delta, China by using anisotropy of magnetic susceptibility. *Marine Geology*, 176, 175–189.
- LIU, K.-B.; SUN, S., and JIANG, X., 1992. Environmental change in the Yangtze River delta since 12,000 years B.P. *Quaternary Research*, 38, 32–45.
- MILLIMAN, J.D. and MEADE, R.H., 1983. World-wide delivery of river sediments to the ocean. *Journal of Geology*, 91, 1–21.
- NAGATA, T., 1961. *Rock Magnetism*. 2nd edition. Tokyo: Maruzen.
- NICHOLS, M. and BIGGS, R., 1985. Estuaries. In: DAVIS, R.A., JR. (ed.), *Coastal Sedimentary Environments*. New York: Springer-Verlag, pp. 77–186.
- PIPER, J.D.A.; ELLIOT, M.T., and KNELLER, B.C., 1996. Anisotropy of magnetic susceptibility in a Paleozoic flysch basin: the Windermere Supergroup, northern England. *Sedimentary Geology*, 106, 235–258.
- READING, H.G., 1996. *Sedimentary Environments: Processes, Facies and Stratigraphy*. 3rd edition. Oxford: Blackwell Scientific Publications.
- REES, A.I., 1965. The use of anisotropy of magnetic susceptibility in the estimation of sedimentary fabric. *Sedimentology*, 4, 257–271.
- REES, A.I. and WOODALL, W.A., 1975. The magnetic fabric of some laboratory-deposited sediments. *Earth and Planetary Science Letters*, 25, 121–130.
- REES, A.I.; VON RAD, U., and SHEPARD, F.P., 1968. Magnetic fabric of sediments from the La Jolla submarine canyon and fan, California. *Marine Geology*, 6, 145–178.
- REINECK, H.-E. and SINGH, I.B., 1980. *Depositional Sedimentary Environments*. Berlin: Springer-Verlag.
- SCHIEBER, J. and ELLWOOD, B.B., 1993. Determination of basinwide paleocurrent patterns in a shale succession from anisotropy of magnetic susceptibility (AMS): a case study of the mid-Proterozoic Newland formation, Montana. *Journal of Sedimentary Petrology*, 63, 874–880.
- STACEY, F.D.; JOPLIN, G., and LINDSAY, J., 1960. Magnetic anisotropy and fabric of some foliated rocks from SE Australia. *Geophysica Pura e Applicata*, 47, 30–40.
- TAIRA, A. and LIENERT, B.R., 1979. The comparative reliability of magnetic, photometric and microscopic methods of determining the orientations of sedimentary grains. *Journal of Sedimentary Petrology*, 49, 759–772.
- TARLING, D.H. and HROUDA, F., 1993. *The Magnetic Anisotropy of Rocks*. London: Chapman & Hall.
- WRIGHT, L.D., 1985. River deltas. In: DAVIS, R.A., JR. (ed.), *Coastal Sedimentary Environments*. New York: Springer-Verlag, pp. 1–76.
- TOKOKAWA, M. and FRANZ, S.-O., 2002. Changes in grain size and magnetic fabric at Blake-Bahama Outer Ridge during the late Pleistocene (marine isotope stages 8–10). *Marine Geology*, 189, 123–144.
- ZIJDERVELD, J., 1976. AC Demagnetization of rocks: analysis of results. In: COLLINSON, D., et al., (eds.), *Methods in Paleomagnetism*. New York: Elsevier, pp. 254–286.